

# **A Review on Mass Transport Phenomena and Factors Affecting the Performance of Thin Film Composite Membrane during Engineered Osmosis Process**

Ahmadreza Zahedipoor, Mehdi Faramarzi, Amir Mansourizadeh,  
Abdolmohammad Ghaedi & Daryoush Emadzadeh\*

Department of Chemical Engineering, Membrane Science and Technology Research Center (MSTRC), Gachsaran Branch, Islamic Azad University, Gachsaran, Iran

Submitted: 05/11/2019. Revised edition: 31/03/2020. Accepted: 02/04/2020. Available online: 16/07/2020

## **ABSTRACT**

Engineered osmosis (EO) is an osmotically driven membrane process that takes advantage of the osmotic pressure gradient to drive water across the semi-permeable membrane from the feed solution (low osmotic pressure) to the draw solution (high osmotic pressure). In the last decade, EO membranes have found various applications in wastewater treatment, seawater/brackish desalination, food processing and power generation. In this paper, the mass transport phenomena of EO processes, driven by concentration gradients, are reviewed. It is followed by reviewing the key factors that affect the separation performance of membrane particularly thin film composite (TFC) membrane during EO operation. Some of the factors reviewed include membrane intrinsic characteristics, filtration orientation, composition of the feed and draw solutions. This mini review is of importance for researchers who would like to start the research work in the field of osmotic membrane developments.

*Keywords:* Thin film composite membrane, Engineered Osmosis, Forward osmosis, pressure retarded osmosis

## **1.0 INTRODUCTION**

During the 1970s, while reverse osmosis (RO) method was widely used for desalination processes, another method known as engineering osmosis (EO) including forward osmosis (FO) and pressure-retarded osmosis (PRO) were introduced to remove salts from saline water [1, 2]. The available literature suggests that the early patents mainly originated from the researchers' opinions rather than experimental findings [3].

EO is an osmotically driven membrane process that takes advantage of the osmotic pressure gradient to drive water across the semi permeable membrane from the feed solution (low osmotic pressure) to the

draw solution (high osmotic pressure) [4]. In the last decade, EO membranes have found various applications in wastewater treatment, seawater/brackish desalination, food processing and power generation [5, 6]. This significance of EO development is greatly attributed to the low energy consumption, low fouling and high water recovery of EO processes in comparison to the pressure-driven membranes such as RO and nanofiltration (NF) membranes. Most of these advantages are resulted from the low hydraulic pressure demand of EO processes [4, 7].

Currently, the most common method for applying a selective layer on a porous support layer is interfacial polymerization (IP) [7, 8]. When two

\* Corresponding to: Daryoush Emadzadeh (email:)  
DOI: <https://doi.org/10.11113/amst.v24n2.174>

immiscible solvents are exposed to each other, the IP process occurs at their interface that is occupied by reactive monomers. Since support layers serve as storage for the active monomers and form the interface for their reactions during the IP process, they have a critical impact on the efficiency of the applied selective layer [9, 10].

Among the monomers, the polyamide (PA) film from IP of 1,3-phenyldiamine (MPD) and 1,3,5-benzenetricarbonyl trichloride (TMC) has drawn the most attention. Due to high water flux, high NaCl and organic rejections, and stability under various operational conditions, PA membranes are extensively used in separation and desalination industries [11, 12]. As a matter of fact, most of the TFC EO membranes that are being produced today are prepared based on PA membranes. As for EO membranes, more than optimizing the skin layer, researchers have concentrated on improving the structure of membranes that are commonly utilized in IP processes [11, 13-15].

The main target of this paper to review the mass transport phenomena of EO processes and the factors affecting the membrane performances during EO operation. This review focuses primarily on new insights into osmotic membrane transport mechanisms and on novel membranes and draw solutions that are currently being developed. Furthermore, the effects of operating conditions on the overall performance of osmotic membranes will be highlighted and future perspectives will be presented.

## 2.0 MASS TRANSPORT PHENOMENA IN ENGINEERED OSMOSIS

Transportation of mass in EO

membranes has a complex mechanism, and its efficiency relies on various variables such as membrane type, structure, and orientation, temperatures and compositions of the feed and draw solutions, and hydraulics. Before discussing about the details of mass transport mechanism, the terms that are used in this paper are reviewed. FO is one of the basics of engineered osmosis which has to work at low hydraulic pressure [16]. In contrast, PRO operates at a high draw solution hydraulic pressure that is termed as transmembrane hydraulic pressure. Transmembrane hydraulic pressure is lower than transmembrane osmotic pressure. This difference allows smooth migration of water from feed to the draw solution as shown in Figure 1 [17, 18].

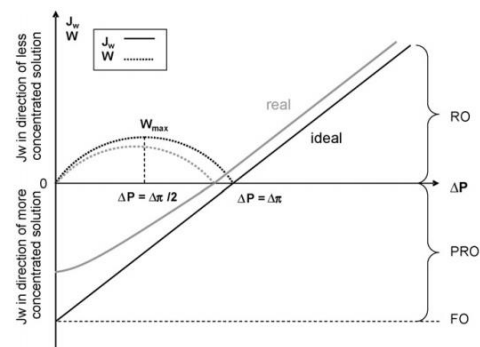


**Figure 1** Direction and magnitude of water flux as a function of applied pressure in FO, PRO, and RO [17, 18]

There are two common trends to evaluate membranes in the EO process. FO mode (also known as FO orientation) is the more popular trend that operates based on exposure between the active layer and the feed solution. The term “active layer facing feed solution” (AL-FS) is also used by some authors to refer to this orientation. In the second trend, which is known as PRO mode (or PRO orientation), or active layer facing draw solution (AL-DS), the active layer is exposed to the draw solution. Figures 2 and 3

compare the differences between FO and PRO mode. During energy recovery process of PRO, the support layer of membrane supplies the mechanical strength that is originated from contact between the active layer and the draw solution. It is worth mentioning that the hydraulic pressure is almost zero during examining membrane in PRO orientation in laboratory scale.

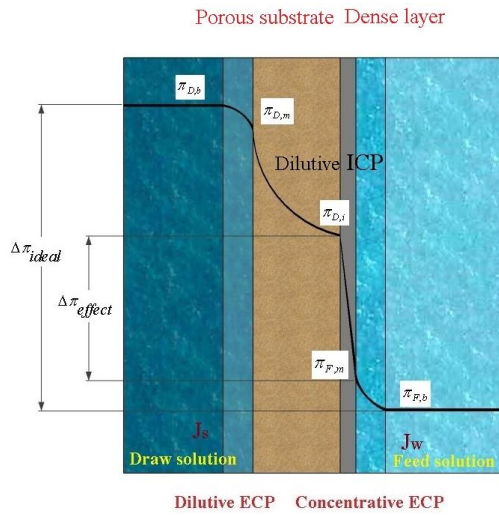


**Figure 2** Schematic diagrams of external and internal concentration polarization developed in FO mode [19]

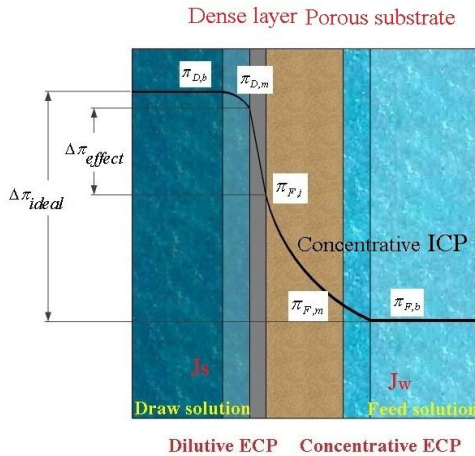


**Figure 3** Schematic diagrams of external and internal concentration polarization developed in PRO mode [19]

The most common models that describe the solute and water flux ( $J_w$ )

in semipermeable membranes are inspired from solution-diffusion and diffusion–convection models. Ideally, the water flux in both FO and PRO orientations is highly dependent on applied hydraulic pressure ( $\Delta P$ ) as well as osmotic pressure difference ( $\Delta\pi$ , constant) across the membrane [20].

$$J_w = A (\Delta\pi - \Delta P)(1)$$

where  $A$  is the water permeability constant ( $m s^{-1}Pa^{-1}$ ), which is an intrinsic characteristic of the membrane. In RO, the components in Equation (1) are reversed (i.e.,  $\Delta P - \Delta\pi$ ). The power generated by a PRO system [20].

$$w = J_w \Delta P = A(\Delta\pi - \Delta P)\Delta P(2)$$

By differentiating Equation (2) with respect to, the power generated ( $w$ ) by PRO is a parabolic function of  $\Delta P$  in which the maximum value is at  $\Delta P = \Delta\pi/2$ . Therefore, it can be concluded that the topmost power that can be generated by PRO system ( $W_{max} = A \Delta\pi^2/4$ ) is a function of water permeability constant and is proportional to the square of the osmotic pressure difference. Equation (3) is used to calculate the salt flux ( $J_s$ ) in FO mode.

$$-J_s = B(\Delta C)(3)$$

where  $B$  and  $\Delta C$  stand for salt permeability coefficient ( $m.s^{-1}$ ) and concentration difference across the membrane selective layer, respectively. Equations (4) and (5) are commonly used to determine the salt permeability coefficient ( $B$ ):

$$B = \frac{A(1-R)(\Delta P - \Delta\pi)}{R} \quad (4)$$

$$R = 1 - \frac{C_p}{C_f} \quad (5)$$

where  $R$  refers to the percentage of salt particles that are sustained in the feed solution, known as the salt rejection,  $C_p$  refers to salt concentration in the permeate, and  $C_f$  stands for the feed solution.

Although the highlighted equations are utilized as models to describe the behavior of solute and solvent fluxes through semipermeable membranes, they are unable to clearly exhibit mass transport in FO due to the concentration polarization phenomena that takes place inside and outside the membrane [21].

### 3.0 PARAMETERS AFFECTING THIN FILM COMPOSITE MEMBRANE

#### 3.1 Support Layer

Quality of the selective skin layer in the surface of membrane highly depends on physicochemical characteristics of the support layer [22]. The support layer of FO membrane should possess the following features: must be thin, must be porous, and must have low tortuosity. The latter one is attributed to the quality of water flux as well as transportation of draw solution solutes into the openings of the active layer. Some recent works were devoted to investigate the performance of a number of membranes in FO applications [23-25].

As one of the most common support layers for conventional TFC FO membranes, polysulfone (PSf) has been used in TFC FO studies by several authors [26]. In one of the prime studies, Yip *et al.* [27] studied the structural parameters ( $S$  value) of the PSf membranes which were prepared by phase inversion. In their work, the support layer was modified in such a way that it improved the

establishment of the selective skin layer. It has been reported that sponge-like shape of the top layer can positively affect the formation of a thin selective skin layer, while the open finger-like structure of pores improves the water flux and diffusion of the leaked salts. They employed the proposed structure and observed the following improvements in performance of the prepared TFC-PSf: lower structural parameter (<500 microns), higher water flux ( $18 \text{ L m}^{-2}\text{h}^{-1}$ ), higher rate of salt rejection (>97%) and tolerating the high pH of an ammonium bicarbonate ( $\text{NH}_3\text{HCO}_3$ ) draw solution. The last feature is the main factor causing the TFC-PSf membranes to outperform asymmetric CA membranes.

Improving hydrophilic features of membranes has been considered as another option to boost their water flux since it raises degree of humidity in pores. In this regard, polyethylene glycol (PEG) and polyvinylpyrrolidone (PVP) have been added to TFC membranes, aiming to meliorate their hydrophilicity and porosity, but it caused reduction in water flux [28, 29]. It was reported that IP step created a dense PA layer inside the pores, which blocked the water flux. In addition, when PEG and PVP molecules exited the TFC membrane, they decreased its stability. In another attempt to improve the hydrophilicity of the PES, Wang *et al.* [22] replaced PEG and PVP with a mixture of polyethersulfone (PES) and sulfonated PSf (sPSf).

A review over the available literature indicates that a reliable method to prepare ideal support layers for FO is lacking. The most accepted morphology is using finger-like pores in the support layer since it provides high diffusion for both salts and water [27]. On the other hand, N. Widjojo [16] and Wang. [17] emphasized on using sponge-like pores in the support

layer as it forms selective skins required for sufficient mechanical support [30, 31]. They studied the impact of membrane structures on their performances in a large scale. They concluded that it is not compulsory to use finger-like pores for securing the low structural parameter required to overcome ICP and improve water flux. More significantly, if the membrane shows high hydrophilic behaviours, the structural parameter may reduce substantially [31].

As another solution, electro-spun PES fibers have been considered as the

support layers for FO TFC membranes as shown in Figure 4 [32, 33]. Authors stated that the resultant substrates exhibited high porosity, low tortuosity, and low structural parameter (80-100 microns) [32]. It was also reported that when the dense layer of the prepared membrane was exposed to the feed (FO configuration); the membrane had acceptable performance up to  $10.5 \text{ mm.s}^{-1}$  water flux (0.5 mol L<sup>-1</sup> NaCl as draw solution).

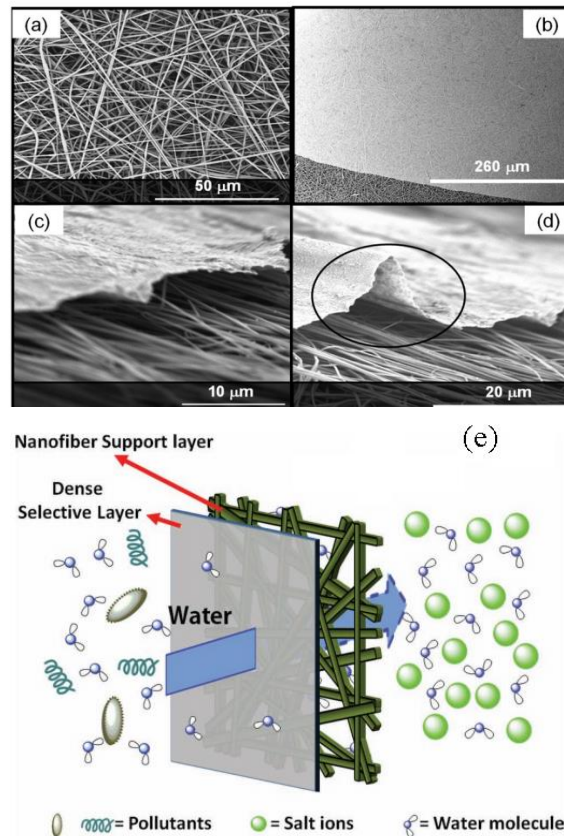


**Figure 4** SEM images of (a) nanofiber PES, (b-d) PES-based TFC polyamide membranes [33], and (e) schematic of an ideal TFC FO membrane with nanofiber support layer [32]

The TFC membranes which benefited from nanofiber support layers showed higher penetrance compared to ones with PES support layers fabricated by phase inversion. Lower structural parameter was the major reason for higher water flux of

nanofiber membranes. While using nanofiber membranes has improved the membrane performance in most cases, still there is uncertainty over the mechanical stability of the selective layers [33]. To overcome this issue, Hoover *et al.* [34] made advantage of

electro-spun nanofiber features in fabricating backing support layers in order to enhance the mechanical stability of the TFC FO membrane. As a result, the mechanical stability of the TFC FO membrane increased at the cost of slight reduction in water diffusion. This modification enabled this class of membranes to deal with real operational conditions where fluid shear forces need to be maintained. The promising finding of such studies has urged researchers to design new membrane structures suitable for industrial osmosis applications. Moreover, electro-spinning the nanofiber support layers can potentially improve their tenable hydrophilic and bactericidal features [35, 36].

### 3.2 Selective Polyamide Skin Layer

The active monomers that are widely used during IP processes are either aliphaticdiamines (e.g. piperazine (PIP), m-phenylenediamine (MPD), and p-phenylenediamine (PPDA)) or acid chlorides (trimesoyl chloride (TMC), isophthaloyl chloride (IPC), 5-chloroformyloxysophthaloyl chloride (CFIC), and 5-isocyanatoisophthaloyl chloride (ICIC)). The MPD–TMC monomer pair has been used in a wide number of studies to prepare selective layers of TFC FO membranes. When pressure is the driving force, the degree of salt rejection and water flux is determined by monomer type's selection. Wei *et al* [37] studied the effect of monomer concentration on the quality of a PA selective layer deposited on a PSf support layer during an IP process. It was reported that concentration of both MPD and TMC had principal influence in PA film formation. A denser PA film structure was obtained by increasing MPD concentration, and increasing TMC concentration increased water

flux at the cost of drop in the degree of cross-linking due to formation of unreacted acyl chloride groups. Enhancing MPD and TMC concentrations had dissimilar effects on FO membranes. Increasing MPD concentration increased water flux, while boosting TMC concentration reduced salt retention. A widely accepted criterion for determining performance of FO membranes is the ratio of water flux or salt reverse flux ( $J_w/J_s$ ) [37].

## 4.0 CONCENTRATION POLARIZATION

Discharge of water from the boundary layer can unbalance the concentration of solution at the membrane–feed interface and the bulk solution. This phenomenon is known as concentration polarization which is common in membrane process [38]. Compared to other processes, concentration polarization takes place more often in FO processes. In FO and PRO mode, concentration polarizations are categorized into two classes: external and internal. The concentration polarization formed inside a membrane support structure is internal concentration polarization (ICP), and the one that occurs at the interface between membrane and liquid is called external concentration polarization (ECP). What separates FO and PRO membranes from the rest of pressure driven membranes is the opposite direction of solute and water fluxes. The ICP that takes place in membranes during FO is originated from two sources: salts discharge which forms dilutive ICP and salt concentration in the porous support layer that is known as concentrative ICP. One of the major consequences of ICP is decline in productivity of FO membranes which is caused by

difference in the effective osmotic pressure ( $\Delta\pi_{\text{eff}}$ ) across the membrane.

ECP can happen on either the interface of the bulk feed of an FO membrane or in its draw solution. Salt preservation by membranes leads to higher solute concentration in the interface between membrane and feed compared to bulk feed solution, a phenomenon known as concentrative ECP. Transportation of water into the draw solution dilutes the solution at the interface between membrane and draw solution, representing an example of dilutive ECP. One of the methods to reduce the chance of ECP occurrence is thinning the boundary layer at the interface between solution and membrane by improving mixing performance [20].

Le *et al.* [20] Equation (6) is not a useful expression for the water flux across a PRO membrane, proposed a model to describe ICP in FO. During developing the model, they considered the impact of salt discharge on the performance of PRO membranes. Since ICP is effects on the osmotic driving force, the term effective osmotic pressure ( $\Delta\pi_{\text{eff}}$ ) was introduced based on which, and the water flux could be studied in more details:

$$J_w = A(\Delta\pi_{\text{eff}} - \Delta P) \quad (6)$$

Reflection coefficient ( $\sigma$ ), another term highly used in pressure driven processes, refers to the ratio of  $\Delta\pi_{\text{eff}}$  to the actual osmotic pressure difference ( $\Delta\pi_{\text{eff}} / \sigma \Delta\pi$ ) [20]. Concentration gradient in the support layer of membrane forms a salt flux, which flows in opposite direction of the convective flow of salts with water. Thus,  $J_s$  can also be written as a function of diffusion and convection

the first and second terms in uation (7), respectively:

$$J_s = D\varepsilon \frac{dC(x)}{dx} - J_w C(x) \quad (7)$$

where D and  $\varepsilon$  refer to salt diffusion coefficient ( $\text{m}^2\text{s}^{-1}$ ) and substrate porosity, respectively. The negative sign on salt flux in this equation indicates that its direction is in the opposite of water flux. Thus,

$$B(C_{D,m} - C_{F,i}) = D\varepsilon \frac{dC(x)}{dx} - J_w C(x) \quad (8)$$

where  $C_{F,i}$  and  $C_{D,m}$  are the salt concentration of the feed solution inside the substrate near the selective layer and the concentration of the draw solution near the membrane surface, respectively. Under the boundary conditions of  $C(x)=C_F$ , mat  $x=0$  and  $C(x)=C_{F,i}$  at  $x=\tau t$ , where  $\tau$  and  $t$  are membrane tortuosity and thickness, Equation (8) can be resolved to

$$\frac{C_{F,i}}{C_{D,m}} = \frac{B[\exp(J_w K) - 1] + J_w \frac{C_{F,m}}{C_{D,m}} \exp(J_w K)}{B[\exp(J_w K) - 1] + J_w} \quad (9)$$

where K is the solute resistivity to salt transport in the porous substrate, which is defined as a function of the structural parameters and the diffusion coefficient D,

$$K = \frac{t\tau}{D\varepsilon} = \frac{S}{D} \quad (10)$$

The ratio of salt concentration is assumed to be approximately equal to the ratio of osmotic pressure:

$$\frac{D\rho_{eff}}{DP} = \frac{\rho_{D,m} - \rho_{F,i}}{\rho_{D,m} - \rho_{F,m}} @ \frac{C_{D,m} - C_{F,i}}{C_{D,m} - C_{F,m}} = \left( \frac{1}{1 - \frac{C_{F,b}}{C_{D,m}}} \right) \left( \frac{1 - \frac{C_{F,b}}{C_{D,m}} \exp(J_w K)}{\frac{B}{J_w} [\exp(J_w K) - 1] + 1} \right) \quad (11)$$

Equations (6) and (11) can be combined to give

$$J_w = A \left[ \left( \frac{C_{D,m} - C_{F,m} \exp(J_w K)}{\frac{B}{J_w} [\exp(J_w K) - 1] + 1} \right) - \Delta P \right] \quad (12)$$

Equation (10) relates water flux in PRO to membrane parameters, once proper flow or stirring conditions are applied, the ECP effect at the feed side of the membrane is suppressed. The concentration at the membrane interface is thus equal to the bulk solution;  $C_{D,m} = C_{D,b}$  and  $C_{F,m} = C_{F,b}$ . Therefore,

$$J_w = A \left[ \left( \frac{C_{D,b} - C_{F,b} \exp(J_w K)}{\frac{B}{J_w} [\exp(J_w K) - 1] + 1} \right) - \Delta P \right] \quad (13)$$

There is no effective direct measurement of the structural parameter (Equation (10)). However, in Equation (14) K can be estimated by measuring the flux when no hydraulic pressure is applied and pure water is used as a feed:

$$K = \frac{1}{J_w} \ln \left( \frac{A\pi_{D,m} - J_w}{B} + 1 \right) \quad (14)$$

Loeb *et al.* [39] introduced a formula to determine K for both FO and PRO membranes under the assumption of ideal solution:

$$K = \left( \frac{1}{J_w} \right) \ln \left( \frac{B + A\pi_{D,m} - J_w}{B + A\pi_{F,b}} \right) \quad (15)$$

By an analysis similar to that in Section A.2 above, we arrive at for PRO mode and

$$K = \left( \frac{1}{J_w} \right) \ln \left( \frac{B + A\pi_{D,b}}{B + J_w + A\pi_{F,m}} \right) \quad (16)$$

for FO mode. Recently, more attention has been given to FO membranes and as a result, more precise models have been introduced [34, 40-47].

#### 4.1 External Concentration Polarization

McCutcheon *et al.* [24, 40, 42, 48] discussed the relationship between flux and polarization in several publications. Their comprehensive models, which were developed based on the boundary layer film theory, took the impact of ECP into account, which was lacking in the previous models [40].

$$\frac{\pi_{F,m}}{\pi_{F,b}} = \exp\left(\frac{J_w}{k}\right) \quad (17)$$

for concentrative ECP in FO mode and

$$\frac{\pi_{D,m}}{\pi_{D,b}} = \exp\left(-\frac{J_w}{k}\right) \quad (18)$$

for dilutive ECP in PRO mode

The mass transfer coefficient parameter ( $k$ ) in Equation (17) and (18) is determined by Sherwood number ( $Sh$ ):

$$k = \frac{ShD}{d_h} \quad (19)$$

In Equation (19),  $D$  and  $d_h$  represent the diffusion coefficient of the solute in draw or feed solution and hydraulic diameter of the flow channel, respectively. It is assumed that the ratio of osmotic pressure at the membrane surface to that in the bulk solution is equivalent to the ratio of concentrations, which is acceptable for dilute solutions based on Van't Hoff's Equation (20). Followings are the most accepted equations for determining Sherwood number in various flow regimes inside a rectangular channel:

$$Sh = 1.85(\text{Re} \cdot \text{Sc} \frac{d_h}{L})^{0.33} \quad (20)$$

(Laminar flow;  $\text{Re} \leq 2100$ ); and (turbulent flow;  $\text{Re} \geq 2100$ )

$$Sh = 0.04 \text{Re}^{0.75} \text{Sc}^{0.33} \quad (21)$$

In Equation (21), where  $\text{Re}$ ,  $\text{Sc}$ , and  $L$  refer to Reynolds number, Schmidt number, and length of the flow channel, respectively. According to Equation (17) and (18), mass transfer coefficient and hydrodynamic conditions of the system have great influence on the ECP model. Alike, various models have been proposed for spiral wound, flat-frame, or tubular module to determine mass transfer coefficient and Sherwood number in different flow conditions [40, 42, 43, 49-54].

## 4.2 Internal Concentration Polarization

Equations (22) and (23) for determining dilutive ICP in FO configuration and concentrative ICP in PRO mode were proposed by McCutcheonin 2007 [40].

$$\frac{\pi_{D,i}}{\pi_{D,b}} = \exp(-J_w K) \quad (22)$$

Dilutive ICP in FO mode and

$$\frac{\pi_{D,i}}{\pi_{D,b}} = \exp(J_w K) \quad (23)$$

Concentrative ICP in PRO mode

The hydraulic pressure parameter is dropped in the following equations to simplify them. Flux equation in FO configuration can be obtained by merging correction factors Equation (17) and Equation (22) into Equation (6):

$$J_w = A(\Delta\pi_{eff} = A(\pi_{D,i} - \pi_{F,m}) = A[\pi_{D,b} \exp(-J_w K) - \Delta\pi_{F,b} \exp\left(\frac{J_w}{k}\right)] \quad (24)$$

By substituting Equation (18) and (23) into (6), flux equation in PRO mode can be obtained:

$$J_w = A(\Delta\pi_{eff} = A(\pi_{D,m} - \pi_{F,i}) = A[\pi_{D,b} \exp\left(\frac{J_w}{k}\right) - \Delta\pi_{F,b} \exp(J_w K)] \quad (25)$$

The main assumption of these equations is absence of ECP effect on porous support layer. Diffusion of water and solute into the porous support layer makes the concentration at the support interface and the concentration in the bulk solution even [48]. The effect of salt permeability

and salt reverse flux in ECP and ICP modules is minimal as their equations are developed based on high salt rejection. Since the new FO membranes can obtain high water flux, the impact of ECP cannot be relinquished any longer [55, 56].

In a novel approach, Achilliet *al.* [18] combined ECP module with Lee's models, and observed that the modified model had better performance in describing flux behavior of osmotic membranes compared to the original Lee's model. This approach was followed by Yip *et al.* who applied ECP, ICP, and reverse salt flux into their flux model (as shown in Equation (26)) to forecast the performance of their PRO membrane [57].

$$J_w = A \left[ \frac{\pi_{D,m} \exp(-\frac{J_w}{k}) - \Delta\pi_{F,b}(J_w K)}{1 + \frac{B}{J_w} [\exp(J_w K) - \exp(-\frac{J_w}{k})]} \right] \quad (26)$$

## 5.0 REVERSE DRAW SOLUTE

Some recent publications have proposed new models to describe solute flux in FO. Direction of solute flux in FO is opposite of direction of water flux, resulting in drop of osmotic pressure driving force, which consequently decreases performance of FO membranes in downstream processes [58]. Moreover, situation can be worsen if there are synchronous solute flux from the feed to the draw solution [59]. In order to migrate from the draw solution to the feed solution, salt flow has to pass three regions (i.e. porous support layer, the dense selective layer and the boundary layer) which are depicted in Figure 5.

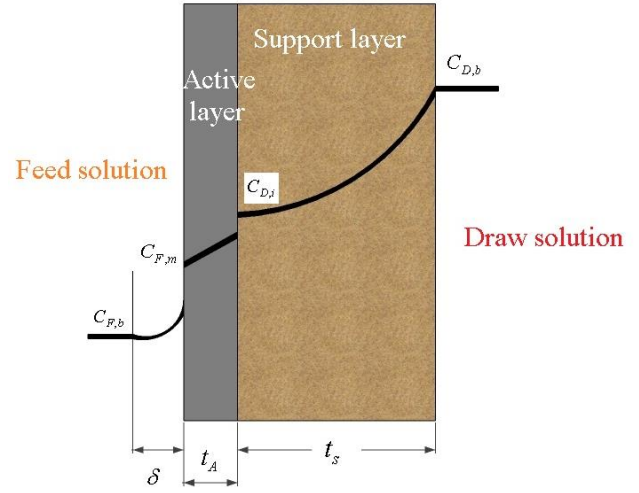


**Figure 5** Profiles of the solute concentration across an asymmetric membrane

The transportation phenomenon in the first and third regions is controlled by both diffusion and convection, but the movement in the dense selective layer is governed solely by diffusion [58]. Transportation of solute across the three regions can be represented by Equation (27):

$$J_s = \frac{J_w (C_{F,b} \exp(Pe^s + Pe^\delta))}{(B \exp(Pe^s) + J_w) \exp(Pe^s) - B} \quad (27)$$

where

$$Pe^s = J_w \frac{t_s \tau}{\varepsilon D} = J_w \frac{S}{D} = J_w k \quad (28)$$

$$Pe^\delta = \frac{J_w}{k} \quad (29)$$

In Equation (28)  $Pe^s$  is the Peclet number in the support layer  $D$  is the binary diffusion coefficient for the solute and water and  $t_s$ ,  $\varepsilon$ , and  $\tau$  are the thickness, porosity, and tortuosity of the support layer, respectively and In Equation (29),  $Pe^\delta$  is the Peclet number of the boundary layer and  $k$  is the feed side mass transfer coefficient,

which can be estimated from a correlation for the rectangular cell geometry and given operating conditions. The term reverse solute flux in Equation (27) should be experimentally determined [60].

It is worth noting that the feature of the fabricated membrane in reverse and forward salt fluxes highly relies on physicochemical characteristics of the draw solute that is used during preparation. Hancock *et al.* [58, 59] studied the impact of various factors such as size, viscosity, and diffusion coefficient of the solutes on reverse salt fluxes. It was found that reverse salt transport can decline the water flux and membrane performance by increasing the chance of concentration polarization and fouling occurrence.

Volume of the produced water per mass of the consumed draw solute can be assumed as the ratio of the water flux to the reverse solute flux. Two separate publications have studied the correlations between that ratio and the process performance [27, 60]:

$$\frac{J_w}{J_s} = \frac{A}{B} \beta R_g T \quad (30)$$

In Equation (30) where  $\beta$  is the Van't Hoff coefficient,  $R_g$  the ideal gas constant, and  $T$  the absolute temperature, respectively. It should be mentioned that although the reverse salt flux selectivity ( $J_w/J_s$ ) is not a function of structural parameters, it is highly related to the water permeability (A) and salt permeability (B), which indirectly makes the reverse salt flux selectivity dependent to the selective layer of the membrane [59]. It's been also reported that the reverse salt flux selectivity does not rely on concentration gradient in the draw solution and operational conditions [27, 59]. As a result, draw solutions

capable of providing high osmotic pressure ( $\beta RT$ ) are desirable [27].

Hancock *et al.* [58, 59] studied the bidirectional mass transport of solutes under various operational conditions for CA membranes and PA TFC membranes. They reported that under similar osmotic driving force, operational conditions and type of solute had significant impacts on the rate of reverse salt flux and water flux, but they seemed to have a minimal effect on the water-salt selectivity ( $J_w/J_s$ ). The highlighted studies were limited to FO processes in the absence of hydraulic pressure. In case of PRO processes, She *et al.* [61] studied the impact of operational conditions on the reverse solute diffusion and the specific solute flux ( $J_s/J_w$ ). They claimed that applying hydraulic pressure increases the ratio of  $J_s/J_w$ , a result that shows Equation (27) has ignored the role of hydraulic pressure on reverse salt flux. Eventually, authors proposed a complimentary equation, which covered all effective parameters Equation (31) as follows:

$$\frac{J_s}{J_w} = \frac{B}{A\beta R_g T} \left(1 - \frac{A\Delta P}{J_w}\right) \quad (31)$$

The increase in the specific reverse solute flux with applied pressure was attributed to the deformation of the commercial membranes used. At high applied pressure, polymer chains of the membrane selective layer may be stretched and pores got enlarged, resulting in the reduced solute rejection. In summary, increased water flux and operating pressure in PRO will always be accompanied by an undesired increase in reverse solute flux.

Membranes with better selectivity (high A/B) are thus greatly desired and should be developed.

## 5.0 CONCLUSIONS

This paper has reviewed the mass transport phenomena and characteristics of TFC membranes for EO application. Factors affecting membrane performance during EO process such as reverse draw solute, membrane fouling and operation conditions have also been covered. This mini review is of importance for researchers in particular for those who want to start experimental work in the field of osmotic membrane research and development.

## REFERENCES

- [1] Y. Zeng, L. Qiu, K. Wang, J. Yao, D. Li, G. P. Simon, R. Wang, H. Wang. 2013. Significantly Enhanced Water Flux in Forward Osmosis Desalination with Polymer-graphene Composite Hydrogels as a Draw Agent. *Rsc Advances*. 3: 887-894.
- [2] F. Zhang, K. S. Brastad, Z. He. 2011. Integrating Forward Osmosis into Microbial Fuel Cells for Wastewater Treatment, Water Extraction and Bioelectricity Generation. *Environmental Science & Technology*. 45: 6690-6696.
- [3] F. Asempour, D. Emadzadeh, T. Matsuura, B. Kruczek. 2018. Synthesis and Characterization of Novel Cellulose Nanocrystals-based Thin Film Nanocomposite Membranes for Reverse Osmosis Applications. *Desalination*. 439: 179-187.
- [4] R. L. McGinnis, M. Elimelech. 2007. Energy requirements of Ammonia-carbon Dioxide Forward Osmosis Desalination. *Desalination*. 207: 370-382.
- [5] J. R. McCutcheon, R. L. McGinnis, M. Elimelech. 2005. A Novel Ammonia-carbon Dioxide Forward (Direct) Osmosis Desalination Process. *Desalination*. 174: 1-11.
- [6] D. Emadzadeh, W. Lau, M. Rahbari-Sisakht, A. Daneshfar, M. Ghanbari, A. Mayahi, T. Matsuura, A. Ismail. 2015. A Novel Thin Film Nanocomposite Reverse Osmosis Membrane with Superior Anti-organic Fouling Affinity for Water Desalination. *Desalination*. 368: 106-113.
- [7] D. Emadzadeh, W. Lau, M. Rahbari-Sisakht, H. Ilbeygi, D. Rana, T. Matsuura, A. Ismail. 2015. Synthesis, Modification and Optimization of Titanate Nanotubes-polyamide Thin Film Nanocomposite (TFN) Membrane for Forward Osmosis (FO) Application. *Chemical Engineering Journal*. 281: 243-251.
- [8] D. Emadzadeh, W. J. Lau, A. F. Ismail. 2013. Synthesis of Thin Film Nanocomposite Forward Osmosis Membrane with Enhancement in Water Flux without Sacrificing Salt Rejection. *Desalination*. 330: 90-99.
- [9] W. Lau, A. F. Ismail, N. Misdan, M. Kassim. 2012. A Recent Progress in Thin Film Composite Membrane: A Review. *Desalination*. 287: 190-199.
- [10] D. Emadzadeh, W. J. Lau, T. Matsuura, A. F. Ismail, M. Rahbari-Sisakht. 2014. Synthesis and Characterization of Thin Film Nanocomposite Forward Osmosis Membrane with Hydrophilic Nanocomposite Support to Reduce Internal Concentration Polarization. *Journal of Membrane Science*. 449:74-85.

- [11] C. A. Nayak, S. S. Valluri, N. K. Rastogi. 2011. Effect of High or Low Molecular Weight of Components of Feed on Transmembrane Flux During Forward Osmosis. *Journal of Food Engineering*. 106: 48-52.
- [12] M. Ghanbari, D. Emadzadeh, W. Lau, S. Lai, T. Matsuura, A. Ismail. 2015. Synthesis and Characterization of Novel Thin Film Nanocomposite (TFN) Membranes Embedded with Halloysite Nanotubes (HNTs) for Water Desalination. *Desalination*. 358: 33-41.
- [13] M. Ghanbari, D. Emadzadeh, W. Lau, T. Matsuura, M. Davoody, A. Ismail. 2015. Super Hydrophilic TiO<sub>2</sub>/HNT Nanocomposites as a New Approach for Fabrication of High Performance Thin Film Nanocomposite Membranes for FO Application. *Desalination*. 371: 104-114.
- [14] M. Ghanbari, D. Emadzadeh, W. Lau, T. Matsuura, A. Ismail. 2015. Synthesis and Characterization of Novel Thin Film Nanocomposite Reverse Osmosis Membranes with Improved Organic Fouling Properties for Water Desalination. *RSC Advances*. 5: 21268-21276.
- [15] M. Ghanbari, D. Emadzadeh, W. Lau, H. Riazi, D. Almasi, A. Ismail. 2016. Minimizing Structural Parameter of Thin Film Composite Forward Osmosis Membranes Using Polysulfone/Halloysite Nanotubes as Membrane Substrates. *Desalination*. 377: 152-162.
- [16] W. J. Lau, S. Gray, T. Matsuura, D. Emadzadeh, J. Paul Chen, A. F. Ismail. 2015. A Review on Polyamide Thin Film Nanocomposite (TFN) Membranes: History, Applications, Challenges and Approaches. *Water Research*. 80: 306-324.
- [17] G.-D. Kang, C.-J. Gao, W.-D. Chen, X.-M. Jie, Y.-M. Cao, Q. Yuan. 2007. Study on Hypochlorite Degradation of Aromatic Polyamide Reverse Osmosis Membrane. *Journal of Membrane Science*. 300: 165-171.
- [18] A. Achilli, T. Y. Cath, A. E. Childress. 2009. Power Generation with Pressure Retarded Osmosis: An Experimental and Theoretical Investigation. *Journal of Membrane Science*. 343: 42-52.
- [19] D. Emadzadeh, W. Lau, T. Matsuura, N. Hilal, A. Ismail. 2014. The Potential of Thin Film Nanocomposite Membrane in Reducing Organic Fouling in Forward Osmosis Process. *Desalination*. 348: 82-88.
- [20] K. Lee, R. Baker, H. Lonsdale. 1981. Membranes for Power Generation by Pressure-retarded Osmosis. *Journal of Membrane Science*. 8: 141-171.
- [21] J. Wei, C. Qiu, C. Y. Tang, R. Wang, A. G. Fane. 2011. Synthesis and Characterization of Flat-sheet Thin Film Composite Forward Osmosis Membranes. *Journal of Membrane Science*. 372: 292-302.
- [22] K. Y. Wang, T. S. Chung, G. Amy. 2012. Developing Thin-film-composite Forward Osmosis Membranes on the PES/SPSf Substrate through Interfacial Polymerization. *AIChE Journal*. 58: 770-781.
- [23] Y. Yu, S. Seo, I.-C. Kim, S. Lee. 2011. Nanoporous Polyethersulfone (PES)

- Membrane with Enhanced Flux Applied in Forward Osmosis Process. *Journal of Membrane Science*. 375: 63-68.
- [24] J. R. McCutcheon, M. Elimelech. 2008. Influence of Membrane Support Layer Hydrophobicity on Water Flux in Osmotically Driven Membrane Processes. *Journal of Membrane Science*. 318: 458-466.
- [25] A. Tiraferri, N. Y. Yip, W. A. Phillip, J. D. Schiffman, M. Elimelech. 2011. Relating Performance of Thin-film Composite Forward Osmosis Membranes to Support Layer Formation and Structure. *Journal of Membrane Science*. 367: 340-352.
- [26] X. Wei, Z. Wang, J. Chen, J. Wang, S. Wang. 2010. A Novel Method of Surface Modification on Thin-Film-Composite Reverse Osmosis Membrane by Grafting Hydantoin Derivative. *Journal of Membrane Science*. 346: 152-162.
- [27] N. Y. Yip, A. Tiraferri, W.A. Phillip, J. D. Schiffman, L. A. Hoover, Y. C. Kim, M. Elimelech. 2011. Thin-film Composite Pressure Retarded Osmosis Membranes for Sustainable Power Generation from Salinity Gradients. *Environmental Science & Technology*. 45: 4360-4369.
- [28] A. K. Ghosh, E. Hoek. 2009. Impacts of Support Membrane Structure and Chemistry on Polyamide–Polysulfone Interfacial Composite Membranes. *Journal of Membrane Science*. 336: 140-148.
- [29] B. Chakrabarty, A. Ghoshal, M. Purkait. 2008. Effect of Molecular Weight of PEG on Membrane Morphology and Transport Properties. *Journal of Membrane Science*. 309: 209-221.
- [30] N. Widjojo, T.-S. Chung, M. Weber, C. Maletzko, V. Warzelhan. 2011. The Role of Sulphonated Polymer and Macrovoid-free Structure in the Support Layer for Thin-film Composite (TFC) Forward Osmosis (FO) Membranes. *Journal of Membrane Science*. 383: 214-223.
- [31] X. Li, K.Y. Wang, B. Helmer, T.-S. Chung. 2012. Thin-film Composite Membranes and Formation Mechanism of Thin-film Layers on Hydrophilic Cellulose Acetate Propionate Substrates for Forward Osmosis Processes. *Industrial & Engineering Chemistry Research*. 51: 10039-10050.
- [32] D. Xiao, C.Y. Tang, J. Zhang, W. C. Lay, R. Wang, A. G. Fane. 2011. Modeling Salt Accumulation in Osmotic Membrane Bioreactors: Implications for FO Membrane Selection and System Operation. *Journal of Membrane Science*. 366: 314-324.
- [33] N.-N. Bui, M. L. Lind, E. Hoek, J. R. McCutcheon. 2011. Electrospun nanofiber Supported Thin Film Composite Membranes for Engineered Osmosis. *Journal of Membrane Science*. 385: 10-19.
- [34] L. A. Hoover, J. D. Schiffman, M. Elimelech. 2013. Nanofibers in Thin-film Composite Membrane Support Layers: Enabling expanded Application of Forward and Pressure Retarded Osmosis. *Desalination*. 308: 73-81.
- [35] L. Chen, L. Bromberg, J. A. Lee, H. Zhang, H. Schreuder-Gibson, P. Gibson, J. Walker, P. T.

- Hammond, T. A. Hatton, G. C. Rutledge. 2010. Multifunctional Electrospun Fabrics Via Layer-by-Layer Electrostatic Assembly for Chemical and Biological Protection. *Chemistry of Materials*. 22: 1429-1436.
- [36] L. F. Greenlee, D. F. Lawler, B. D. Freeman, B. Marrot, P. Moulin. 2009. Reverse Osmosis Desalination: Water Sources, Technology, and Today's Challenges. *Water Research*. 43: 2317-2348.
- [37] J. Wei, X. Liu, C. Qiu, R. Wang, C. Y. Tang. 2011. Influence of Monomer Concentrations on the Performance of Polyamide-based Thin Film Composite Forward Osmosis Membranes. *Journal of Membrane Science*. 381: 110-117.
- [38] S. Sablani, M. Goosen, R. Al-Belushi, M. Wilf. 2001. Concentration Polarization in Ultrafiltration and Reverse Osmosis: A Critical Review. *Desalination*. 141: 269-289.
- [39] S. Loeb, L. Titelman, E. Korngold, J. Freiman. 1997. Effect of Porous Support Fabric on Osmosis through a Loeb-Sourirajan Type Asymmetric Membrane. *Journal of Membrane Science*. 129: 243-249.
- [40] J. R. McCutcheon, M. Elimelech. 2007. Modeling Water Flux in Forward Osmosis: Implications for Improved Membrane Design. *AIChE Journal*. 53: 1736-1744.
- [41] M. Reali, G. Dassie, G. Jonsson. 1990. Computation of Salt Concentration Profiles in the Porous Substrate of Anisotropic Membranes Under Steady Pressure-Retarded-Osmosis Conditions. *Journal of Membrane Science*. 48: 181-201.
- [42] J. R. McCutcheon, M. Elimelech. 2006. Influence of Concentrative and Dilutive Internal Concentration Polarization on Flux Behavior in Forward Osmosis. *Journal of Membrane Science*. 284: 237-247.
- [43] C. H. Tan, H. Y. Ng. 2008. Modified Models to Predict Flux Behavior in Forward Osmosis in Consideration of External and Internal Concentration Polarizations. *Journal of Membrane Science*. 324: 209-219.
- [44] M. Park, J. J. Lee, S. Lee, J. H. Kim. 2011. Determination of a Constant Membrane Structure Parameter in Forward Osmosis Processes. *Journal of Membrane Science*. 375: 241-248.
- [45] C. Y. Tang, Q. She, W. C. Lay, R. Wang, R. Field, A. G. Fane. 2011. Modeling Double-skinned FO Membranes. *Desalination*. 283: 178-186.
- [46] N. T. Hancock, P. Xu, D. M. Heil, C. Bellona, T. Y. Cath. 2011. Comprehensive Bench-and Pilot-scale Investigation of Trace Organic Compounds Rejection by Forward Osmosis. *Environmental Science & Technology*. 45: 8483-8490.
- [47] C. Y. Tang, Q. She, W. C. Lay, R. Wang, A. G. Fane. 2010. Coupled Effects of Internal Concentration Polarization and Fouling on Flux Behavior of Forward Osmosis Membranes During Humic Acid Filtration. *Journal of Membrane Science*. 354: 123-133.
- [48] J. R. McCutcheon, R. L. McGinnis, M. Elimelech. 2006. Desalination by Ammonia-carbon Dioxide Forward Osmosis: Influence of Draw and Feed Solution Concentrations on Process Performance. *Journal of*

- Membrane Science*. 278: 114-123.
- [49] A. Achilli, T. Y. Cath, A. E. Childress, 2009. Power Generation with Pressure Retarded Osmosis: An Experimental and Theoretical Investigation. *Journal of Membrane Science*. 343: 42-52.
- [50] B. Gu, D. Kim, J. Kim, D. Yang. 2011. Mathematical Model of Flat Sheet Membrane Modules for FO Process: Plate-and-frame Module and Spiral-wound Module. *Journal of Membrane Science*. 379: 403-415.
- [51] G. Schock, A. Miquel. 1987. Mass Transfer and Pressure Loss in Spiral Wound Modules. *Desalination*. 64: 339-352.
- [52] V. Gekas, B. Hallström. 1987. Mass Transfer in the Membrane Concentration Polarization Layer Under Turbulent Cross Flow: I. Critical literature Review and Adaptation of Existing Sherwood Correlations to Membrane Operations. *Journal of Membrane Science*. 30: 153-170.
- [53] E. M. Hoek, A. S. Kim, M. Elimelech. 2002. Influence of Crossflow Membrane Filter Geometry and Shear Rate on Colloidal Fouling in Reverse Osmosis and Nanofiltration Separations. *Environmental Engineering Science*. 19: 357-372.
- [54] M. C. Wong, K. Martinez, G. Z. Ramon, E. Hoek. 2012. Impacts of Operating Conditions and Solution Chemistry on Osmotic Membrane Structure and Performance. *Desalination*. 287: 340-349.
- [55] Y. Xu, X. Peng, C. Y. Tang, Q. S. Fu, S. Nie. 2010. Effect of Draw Solution Concentration and Operating Conditions on Forward Osmosis and Pressure Retarded Osmosis Performance in a Spiral Wound Module. *Journal of Membrane Science*. 348: 298-309.
- [56] C. Y. Tang, Q. She, W. C. L. Lay, R. Wang, A. G. Fane. 2010. Coupled Effects of Internal Concentration Polarization and Fouling on Flux Behavior of Forward Osmosis Membranes during Humic Acid Filtration. *Journal of Membrane Science*. 354: 123-133.
- [57] N. Y. Yip, A. Tiraferri, W. A. Phillip, J. D. Schiffman, M. Elimelech. 2010. High Performance Thin-film Composite Forward Osmosis Membrane. *Environmental Science & Technology*. 44: 3812-3818.
- [58] N. T. Hancock, W. A. Phillip, M. Elimelech, T. Y. Cath. 2011. Bidirectional Permeation of Electrolytes in Osmotically Driven Membrane Processes. *Environmental Science & Technology*. 45: 10642-10651.
- [59] N. T. Hancock, T. Y. Cath. 2009. Solute Coupled Diffusion in Osmotically Driven Membrane Processes. *Environmental Science & Technology*. 43: 6769-6775.
- [60] J. S. Yong, W. A. Phillip, M. Elimelech. 2012. Coupled Reverse Draw Solute Permeation and Water Flux in Forward Osmosis with Neutral Draw Solutes. *Journal of Membrane Science*. 392: 9-17.
- [61] Q. She, X. Jin, C. Y. Tang. 2012. Osmotic Power Production from Salinity Gradient Resource by Pressure Retarded Osmosis: Effects of Operating Conditions and Reverse Solute Diffusion. *Journal of Membrane Science*. 401-402: 262-273.

**LIST OF ABBREVIATIONS**

Sc	-	Schmidt number
Sh	-	Sherwood number
C <sub>p</sub>	-	Concentration polarization
CTA	-	Cellulose triacetate
DMF	-	Dimethylformamide
DMSO	-	Dimethyl sulfoxide
ECP	-	External concentration polarization
FO	-	Forward Osmosis
FTIR	-	Fourier Transform Infrared Spectroscopy
HTI	-	Hydration Technologies Inc
ICP	-	Internal concentration polarization
IPC	-	Isophthaloyl chloride
M <sub>w</sub>	-	Molecular weight
NF	-	Nanofiltration
PA	-	Polyamide
PAI	-	Polyamide-imide
PAN	-	Polyacrylonitrile
PAS	-	Positron annihilation spectroscopy
PC	-	Phthaloyl chloride
PDA	-	Phenylenediamine
PEG	-	Polyethylene Glycol
PEI	-	Polyethyleneimine
PES	-	Polyether sulfone
PI	-	Polyimide
PIP	-	Piperazine
PRO	-	Pressure retarded osmosis
PSf	-	Polysulfone
PS	-	Polystyrene
PSS	-	Poly(sodium 4-styrene-sulfonate)
PVP	-	Polyvinylpyrrolidone
PRO	-	Pressure-retarded osmosis
PVP	-	Polyvinylpyrrolidone
Re	-	Reynolds number
RO	-	Reverse osmosis
SEM	-	Scanning Electron Microscope
SDS	-	Sodium dodecyl sulfate
sPEEK	-	Sulfonated poly(ether ether ketone)
sPSf	-	Sulfonated polyethersulfone
TFC	-	Thin-film composite
TEA	-	Triethylamide
TMC	-	Trimesoyl chloride
TPC	-	Terephthaloyl chloride
UF	-	Ultrafiltration

**LIST OF SYMBOLS**

A	-	Water permeability coefficient ( $\text{m}^3/\text{m}^2 \cdot \text{s} \cdot \text{Pa}$ )
B	-	Solute permeability coefficient (m/s)
C	-	Concentration of salt (mol/l)
$C_{F,b}, C_{D,b}$	-	Salt concentration of the bulk feed and draw solution
$C_{F,i}, C_{D,i}$	-	Concentration of feed and draw solution near membranesurface inside porous supports
$C_{F,m}, C_{D,m}$	-	Concentration of feed and draw solution near membranesurface
$C_p, C_f$	-	Salt concentration in permeate and feed solutions dh hydraulicdiameter (m)
D	-	Solute diffusion coefficient ( $\text{m}^2 \text{s}^{-1}$ )
$D_o$	-	The diffusion coefficient at an infinite dilution ( $\text{m}^2\text{s}^{-1}$ )
$D_e$	-	Effective diffusion coefficient ( $\text{m}^2\text{s}^{-1}$ )
$d_p$	-	pore diameter (nm)
$d_s$	-	Solute diameter (nm)
$D_s$	-	Diffusion coefficient of salt in the membrane substrate ( $\text{m}^2 \cdot \text{s}^{-1}$ )
IP	-	Interfacial polymerization
$J_s$	-	Reverse salt flux ( $\text{g m}^{-2} \text{h}^{-1}$ )
$J_w$	-	Water flux ( $\text{m}^3\text{m}^{-2} \text{s}^{-1}$ )
K	-	Water transport coefficient ( $\text{m} \cdot \text{s}^{-1}$ )
$K_b$	-	Mass-transfer coefficient ( $\text{m} \cdot \text{s}^{-1}$ )
$K_d$	-	Mass-transfer coefficient ( $\text{m} \text{ s}^{-1}$ )
$K_c$	-	Mean mass transfer coefficient ( $\text{m} \cdot \text{s}^{-1}$ )
$K^*$	-	Solute resistance coefficient independent of diffusivity
$K_m$	-	Solute diffusion resistivity within the porous layer ( $\text{s m}^{-1}$ )
L/t	-	Thickness ( $\mu\text{m}$ )
M	-	Molality (M)
MWCO	-	Molecular weight cut-off (kDa)
P	-	Pressure (bar)
q	-	Material density ( $\text{g} \cdot \text{cm}^{-3}$ )
R	-	Solute rejection (%)
S	-	Membrane structural parameter (m)
T	-	Membrane thickness (m)
$V_w$	-	Partial molar volume of water ( $\text{m}^3\text{s}^{-1}$ )
W	-	Power ( $\text{W}/\text{m}^2$ )
$W_d$	-	Dry membrane weight (g)
$W_w$	-	Wet membrane weight (g)

**GREEK LETTERS**

$\pi$	-	Osmotic pressure (Pa)
$\pi_{F,b}, \pi_{D,b}$		-Osmotic pressure of the bulk feed and draw solution (Pa)
$\pi_{F,m}, \pi_{D,m}$		-Osmotic pressure of feed and draw solution near membranesurface (Pa)
$\pi_{F,i}, \pi_{D,i}$		-Osmotic pressure of feed and draw solution near membranesurface inside porous supports (Pa)
$\Delta P$	-	Osmotic pressure (bar)
$\Delta\pi, \Delta\pi_{eff}$		-Osmotic pressure difference and effective osmotic pressuredifference (Pa)
$\varepsilon$	-	Membrane porosity
$\sigma$	-	Reflection coefficient
$\tau$	-	Pore tortuosity
$\eta_w, \eta_s$	-	Viscosity of water and solution ( $\text{kg m}^{-1}\text{s}^{-1}$ )
$\mu$	-	Chemical potential
$\gamma$	-	Activity coefficient